

A STUDY OF VISCOUS FLOW OVER ELLIPTIC CYLINDERS

Ravi Bahl
 Mechanical Engineering Department
 Technical Teachers' Training Institute
 Chandigarh, India

Abstract

Numerical solutions of Navier Stokes equations for steady, incompressible, laminar flow of viscous fluid over elliptical cylinders are obtained. The steady state Navier Stokes equations are written in elliptic coordinate system, and recast in terms of vorticity and 'disturbance stream function'. These equations are put in their finite difference form and solved by a modified version of extrapolated Liebmann method. In this modified and updated version a new set of far away boundary conditions have been developed, in addition a good distribution of grid points have been obtained without involving any transformation. Solutions are obtained in terms of important flow parameters for Reynolds number varying from 15 to 50 and thickness ratio of elliptic cylinders varying from approximately 25% to 100%.

solutions and vortex shedding. Some workers^(6,23-26) have done extensive experimental work for incompressible steady flow over circular cylinders.

Numerical solutions of Navier Stokes equations are obtained by Jordan and Fromm⁽²⁷⁾ using SOR method of Liebmann; method of series and truncation is used by Patel⁽²⁸⁾; Fornberg^(4,29) has developed a technique based on Newton's method which is second order accurate. Lately fast poisson solver technique has been developed and used by Temperton⁽³⁰⁾, Fornberg⁽⁴⁾ and Berger⁽³¹⁾. This technique has proved to be faster but its use is so far limited to lower values of Reynolds numbers. Berger⁽³¹⁾ observed errors in the original technique in surface values and modified the technique to eliminate these errors.

I.

Introduction

For incompressible fluids, Navier Stokes equation is of the form:

$$\rho \frac{D\vec{q}}{Dt} = \rho \vec{F} - \nabla p + \mu \nabla^2 \vec{q} \quad (1.1)$$

In conjunction with continuity equation

$$\nabla \cdot \vec{q} = 0 \quad (1.2)$$

One obtains four equations for the three velocity components u,v,w and the pressure p.

Study of flow over elliptic cylinders has been done by few workers⁽¹⁻⁵⁾. This study is done by use of unsteady state Navier Stokes equations at low and moderate values of Reynolds numbers. In most of the work, investigations are carried out on the starting flow and development of lift and drag at angles of attack. Influence of surface boundary conditions on flow characteristic is examined.

The study of flow over circular cylinders has been done by a large number of workers in the last thirty five years. The study being directed towards: understanding of fluid flow; development of newer experimental methods; improving accuracy of available results; development of asymptotic theories; determination and addition of new results and so on.

Steady state⁽⁶⁻¹⁴⁾ Navier Stokes equations and unsteady⁽¹⁵⁻²²⁾ Navier Stokes equations are solved numerically for flow over circular cylinders to obtain steady state

Peregrine⁽³²⁾ has made certain comments on the theoretical predictions and calculations of Fornberg^(4,29) and Smith^(33,34). He observes that certain parameters such as surface shear, pressure distribution, point of separation and drag values are predicted with reasonable accuracy by use of coarser meshes, but to predict eddy characteristic accurately very fine mesh has to be used. In the wind tunnel experiments Smith has established that eddy characteristics are extremely sensitive to the proximity of walls and wind tunnel experiments do not replicate flows corresponding to unbounded fluid domains. Numerical solutions of flow problems require a grid distribution in a manner as would give a dense distribution of points in regions where functions are apt to quicker variations and lesser points in regions of well behaved functions. The works of Thoman and Szweczyk⁽¹⁹⁾, Fornberg^(4,29) and Ghia⁽³⁵⁾ at all need special mention. They use an extensive grid system with a large number of grid points in the wake and near the surface. Thus their results give a good picture of eddy characteristics, though with prohibitive computer time and money.

A study of Imai's asymptotic solutions⁽³⁶⁾ for flow over circular cylinder indicates that disturbance in streamfunction and vorticity value and their variations are non-zero in the wake. The fact has been made use of in solutions of steady state Navier Stokes (elliptic) equations by Keller and Takami⁽¹¹⁾ and Fornberg^(4,29). The problem of imposing correct downstream boundary conditions has been bypassed

III. Mathematical Foundation

by a host of workers by use of unsteady Navier Stokes equations (which are parabolic). In the upstream of the disturbance(wake) the flow conditions are not identical. Thus there is need to handle downstream boundary conditions in a special manner. The mixed type of boundary conditions are most suitable and this has been established by Fornberg^(14,29).

The type of computers needed for extensive and accurate numerical work as done by Forberg^(14,29) are CDC STAR 100, CDC Cyber 205, UNIVAC Illiac IV and Goodyear Staren IV.

II. Problem Statement

Incompressible, steady state Navier Stokes equations are written for two dimensional flow in elliptic coordinate system. Symmetry of flow is imposed about the major axis of elliptical cylinder. The equations are first written in terms of vorticity and stream function. Concept of disturbance stream function is introduced and the equations are written in terms of vorticity and disturbance stream function. Expressions are formulated for value of stream function, velocity, vorticity, pressure distribution on the surface and drag coefficient in terms of vorticity and disturbance stream function.

Search has been made for the type of boundary conditions (far away). The nature of boundary conditions was decided after critical examination of the analytic asymptotic solutions for circular cylinder and some numerical experimentation by the author.

The stream function and vorticity equations and various expressions are put in their finite difference form. The finite difference equations are solved by a modified version of Liebmann method by successive over relaxation. The process of the iteration is continued till changes in values of vorticity and stream function do not exceed some pre-assigned small value.

Numerical experimentation has been validated by solving Navier Stokes equations for flow over elliptic cylinder having thickness ratio of 99.93%, and comparing the results obtained with results for flow over circular cylinders. Results show good agreement for coefficient of drag angle of separation, vorticity and pressure distribution over the surface. Further experimentation is done to obtain results for 75.09% elliptic cylinder, 50.05% elliptic cylinder and 24.96% elliptic cylinder.

A. Differential Equations and Boundary Conditions.

Equations 1.1, and 1.2, are written in terms of disturbance stream function ψ and vorticity ω . The flow parameters are non-dimensionalised with reference to the free stream velocity U ; and geometric parameters wrt half major axis 'a'; shear stress and pressure are non-dimensionalised wrt dynamic head $\frac{1}{2}\rho U^2$; so that Reynolds number is defined by $Re = Ua/\nu$, total stream function Ψ , is given by $\Psi = y + \psi$. The continuity equation 1.2 is identically satisfied by the stream function ψ . Further equation 1.1 with little mathematical manipulation becomes the vorticity transport equations and in elliptic coordinate system, i.e, in (ξ, η) coordinate system is written as:

$$\frac{\partial \psi}{\partial \eta} \frac{\partial \omega}{\partial \xi} - \frac{\partial \psi}{\partial \xi} \frac{\partial \omega}{\partial \eta} + \frac{\sinh \xi \cosh \eta}{\cosh \xi_0} \frac{\partial \omega}{\partial \xi} - \frac{\cosh \xi \sinh \eta}{\cosh \xi_0} \frac{\partial \omega}{\partial \eta} = \frac{2}{Re} \left(\frac{\partial^2 \omega}{\partial \xi^2} + \frac{\partial^2 \omega}{\partial \eta^2} \right) \quad (2.1)$$

and vorticity equation is written as

$$\omega = -\frac{1}{h^2} \left(\frac{\partial^2 \psi}{\partial \xi^2} + \frac{\partial^2 \psi}{\partial \eta^2} \right) \quad (2.2)$$

where h is metric coefficient for elliptic coordinate system and given by

$$h = \sqrt{\sinh^2 \xi + \sin^2 \eta} / \cosh \xi_0 \quad (2.3)$$

The velocity components u and v in direction ξ and η are given by

$$u = \frac{1}{h} \left(\frac{\partial \psi}{\partial \eta} + \frac{\partial \psi}{\partial \eta} \right), \quad v = -\frac{1}{h} \left(\frac{\partial \psi}{\partial \xi} + \frac{\partial \psi}{\partial \xi} \right) \quad (2.4)$$

where $\xi = \xi_0$ represents surface of the elliptical cylinder, pressure p is given by

$$p = \frac{4}{Re} \int_0^{\eta} \left(\frac{\partial \omega}{\partial \xi} \right)_{\xi_0} d\eta \quad (2.5)$$

$$f = \sqrt{\sin^2 \eta + \cos^2 \eta \tanh^2 \xi_0} \quad (2.6)$$

Coefficient of drag due to pressure

$$C_{dp} = - \int_0^{\pi} p f \cos \theta d\eta \quad (2.7)$$

coefficient of drag due to friction

$$C_{df} = \frac{4}{Re} \int_0^{\pi} \omega f \sin \theta d\eta \quad (2.8)$$

Total coefficient of drag: $C_{dp} + C_{df} = C_d$
 where θ is angle made by normal at a point on surface with x-axis.

Equations 2.1 and 2.2 are two second order partial differential equations in two unknowns ψ and ω therefore specification of both ψ and ω or their normal derivatives is required on all boundaries. The graphical representation of flow problem is shown in fig. 1. The boundary conditions specified are:

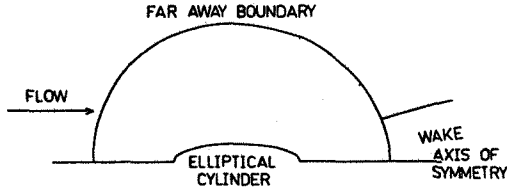


FIG 1 BOUNDARY CONDITIONS

1. On the surface of the elliptical cylinder no slip conditions exist and normal component of velocity on the surface is zero, i.e, impervious surface.
2. On the axis of symmetry both disturbance stream function and vorticity are zero.
3. On the far away boundary both disturbance stream function and vorticity are zero except in wake region. On the wake portion of boundary the value of disturbance stream function and vorticity are extrapolated from interior values by a smooth curve.

B. Finite Difference Form

$$\psi_{i,j}^{n+1} = \psi_{i,j}^n + \frac{\alpha'}{CF} \left\{ \psi_{i+1,j}^n + \psi_{i-1,j}^n + \frac{1}{c^2} (\psi_{i,j+1}^n + \psi_{i,j-1}^n) - A \psi_{i,j}^n + (\Delta \xi)^2 h_{i,j}^2 \omega_{i,j}^n \right\}$$

$$\omega_{i,j}^{n+1} = \omega_{i,j}^n + \frac{\beta'}{CF} \left\{ (1+c_1 c_\xi) \omega_{i+1,j}^{n+1} + (1+c_2 c_\xi) \omega_{i-1,j}^n + \left(\frac{1}{c^2} + c_4 c_\eta\right) \omega_{i,j+1}^n + \left(\frac{1}{c^2} + c_5 c_\eta\right) \omega_{i,j-1}^{n+1} - (A+c_3 c_\xi + c_6 c_\eta) \omega_{i,j}^n \right\}$$

$$\text{parameter CF} = \frac{1}{2 \left[\frac{1}{c^2} \left(1 + \frac{1}{c^2}\right) + |c_\xi| + |c_\eta| \right]}$$

where τ is a factor less than 2, in the present scheme its value was taken as 1.9 according to stability criteria

α', β' = modified relaxation parameters chosen after numerical experimentation

also value of $\frac{\alpha'}{CF}, \frac{\beta'}{CF}$ lies between 1/4 and 1/2 where for

$$c_\xi \leq 0; \quad c_1 = -1; \quad c_2 = 0; \quad c_3 = c_1 + c_2$$

$$c_\eta \leq 0; \quad c_4 = -1; \quad c_5 = 0; \quad c_6 = c_4 + c_5$$

$$c_\xi > 0; \quad c_1 = 0; \quad c_2 = 1; \quad c_3 = c_1 + c_2$$

$$c_\eta > 0; \quad c_4 = 0; \quad c_5 = 1; \quad c_6 = c_4 + c_5$$

and for

$$u' = \frac{1}{h} \frac{\partial \psi}{\partial \eta}, \quad c = \Delta \eta / \Delta \xi, \quad v' = -\frac{1}{h} \frac{\partial \psi}{\partial \xi}$$

$$c_\xi = \frac{Re \Delta \xi}{2} (h_{1,j} u'_{1,j} + \frac{\sinh \xi \cos \eta}{\cosh \xi_0})$$

$$c_\eta = \frac{Re \Delta \eta}{2} (h_{1,j} v'_{1,j} - \frac{\cosh \xi \sin \eta}{\cosh \xi_0})$$

$$A = 2 \left[1 + (\Delta \xi / \Delta \eta)^2 \right]$$

The boundary conditions in the finite difference form are

a) on the surface of the elliptical

$$\xi = \xi_0; \quad i=1, j=1, 2, \dots, q$$

$$\psi_{1,j} = \tanh \xi_0 \sin \eta_j$$

$$\omega_{i,j} = -\frac{1}{h_{i,j}} \left\{ \frac{2}{(\Delta \xi)^2} \psi_{2,j} + \left[1 + \frac{2}{(\Delta \xi)^2} \right] \tanh \xi_0 \sin \eta_j + \frac{2}{\Delta \xi} \sin \eta_j \right\}$$

b) on the axis of symmetry

i) Ahead of elliptical cylinder

$$\psi_{i,p} = 0$$

$$\omega_{i,p} = 0$$

$$i=1, 2, 3, \dots, p$$

ii) Behind the elliptical cylinder

$$\psi_{i,1} = 0$$

$$\omega_{i,1} = 0$$

$$i=1, 2, 3, \dots, p$$

c) On the far away boundary

i) Except in the wake: $\psi_{p,j} = 0, \omega_{p,j} = 0$

IV. NUMERICAL EXPERIMENTATION⁽³⁷⁾

In this iteration scheme all second order derivatives are replaced by central differences, first order derivatives of disturbance stream function are replaced by central differences, and first order derivatives of vorticity are replaced by forward difference or backward difference depending on the sign of their coefficients. The iteration is continued till the latest value ψ^n differs from previous value ψ^{n-1} by less than 10^{-5} and latest value ω^{n+1} differs from previous value ω^n by less than 10^{-5} at all mesh points.

Computations are first carried out for 99.93% elliptic cylinder at $Re = 15$ using a grid of 21×11 . The far away boundary was at about $8a$. The boundary was then shifted to $10a$, with some improvements in flow parameters, but no separation. A grid of 46×21 was used, the flow parameters agreed with existing values. Further a grid of 56×21 was used with boundary shifting to $20a$. The results showed good agreement with existing results for circular cylinders. Further runs were made at $Re = 30$ and 50 for 99.93% elliptic cylinder. These results also compared well with existing results for circular cylinders. At $Re = 100$ the values of drag coefficient and surface vorticity were lower due to the coarse grid. No difficulty was encountered in convergence of iterative scheme. A finer mesh was not used due to limits of computer time.

V. RESULTS AND DISCUSSIONS

Result of the computational investigation have been presented and discussed in the following text.

Validation of Computational Technique:

The governing equations in their finite difference form are computationally well posed as determined by numerical experimentation. The 99.93% elliptical cylinders bear close geometrical approximation with circular cylinders and as such solutions were first obtained for incompressible, viscous steady flow past 99.93% elliptical cylinder at Reynolds number of 15, 30 and 50.

These computed results were compared with available existing results. Comparisons were made for flow parameters such as drag coefficient, figure 2; vorticity distribution, figure 9; pressure distribution, figure 10; and angle of separation. There is a good agreement.

Solutions were subsequently obtained for 75.09%, 50.05%, 24.96% elliptical cylinders at Reynolds number of 15, 30 and 50 using the same technique and same computer programme but altering the input data only.

Discussion on Coefficient of drag.

Coefficient of drag as obtained in the present work for 99.93% elliptic cylinder has been compared with available values of drag for circular cylinders. This comparison is shown in figure 2. Figures 2-5 show that for each elliptic cylinder the drag coefficient decreases with increase in Reynolds number. Important flow characteristics as obtained in present work are given in table I.

It is observed that at each of Reynolds number (see fig.6-8) of 15, 30 and 50 the drag coefficients C_d , C_{dp}

increase with increase in thickness ratio while drag coefficient due to friction C_{df}

decreases by a very small amount due to increase in thickness ratio. This decrease is more below 25% thickness ratio and the tends to even out as thickness ratio increases.

One of the important findings of the present research is that coefficient of drag C_d increases linearly with increase

in thickness ratio for a given value of Reynolds number. This linear behaviour is observed for thickness ratio greater than 25% and has now been expressed in terms of a 'drag thickness ratio law'.

$$C_{d_x} = C_d - 0.0051(100-x) \text{ for a given value of } Re,$$

where,

C_d = Coefficient of drag for circular cylinder.

C_{d_x} = Coefficient of drag for x% elliptical cylinder.

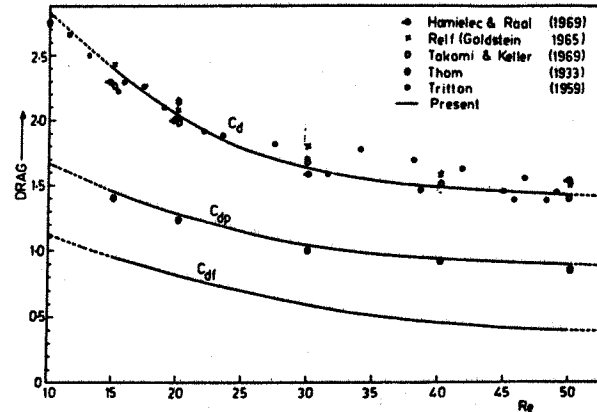


FIG 2 EFFECT OF REYNOLDS NUMBER ON DRAG 99.93% ELLIPSE

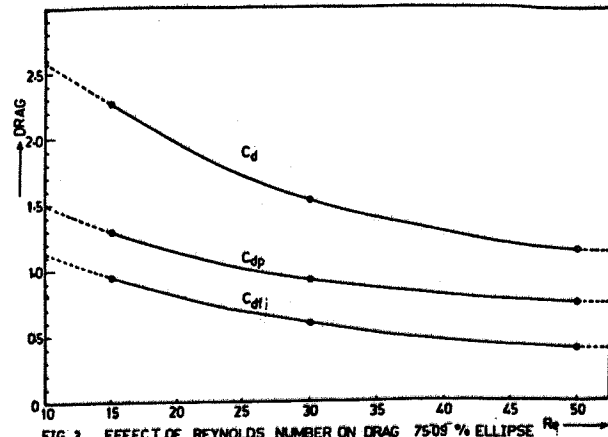


FIG 3 EFFECT OF REYNOLDS NUMBER ON DRAG 75.09% ELLIPSE

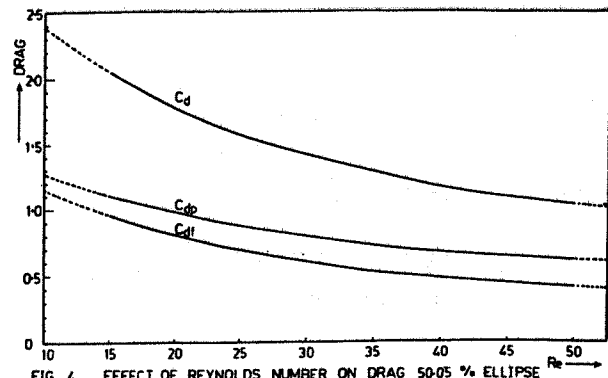


FIG 4 EFFECT OF REYNOLDS NUMBER ON DRAG 50.05% ELLIPSE

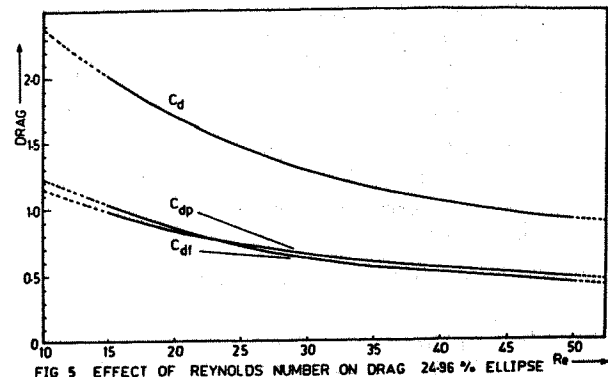


FIG 5 EFFECT OF REYNOLDS NUMBER ON DRAG 24.96% ELLIPSE

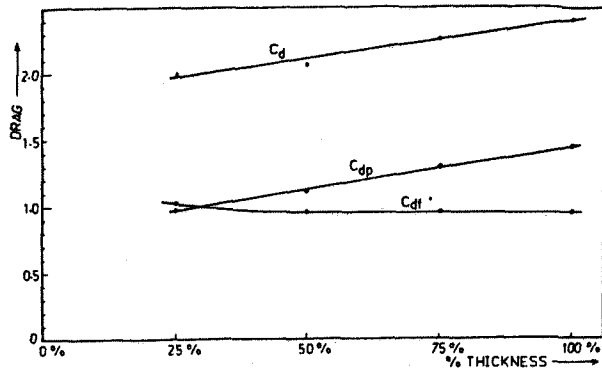


FIG 6 EFFECT OF THICKNESS ON DRAG AT Re=15

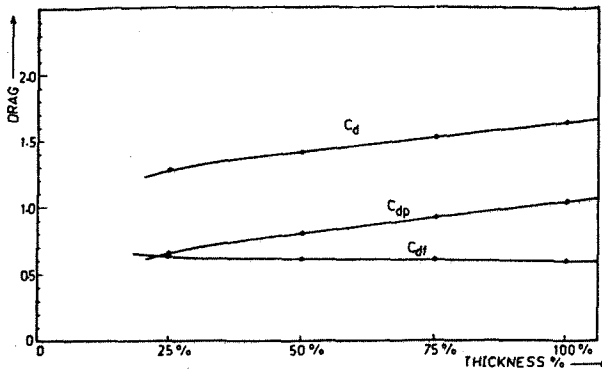


FIG 7 EFFECT OF THICKNESS ON DRAG AT Re=30

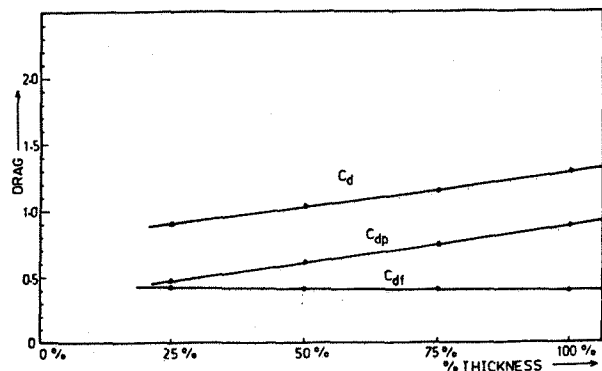


FIG 8 EFFECT OF THICKNESS ON DRAG AT Re=50

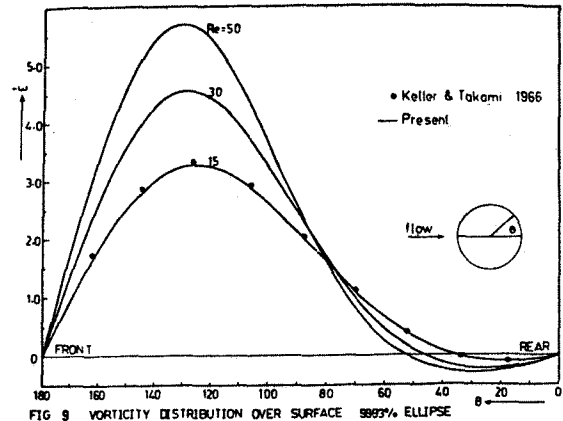


FIG 9 VORTICITY DISTRIBUTION OVER SURFACE 99.93% ELLIPSE

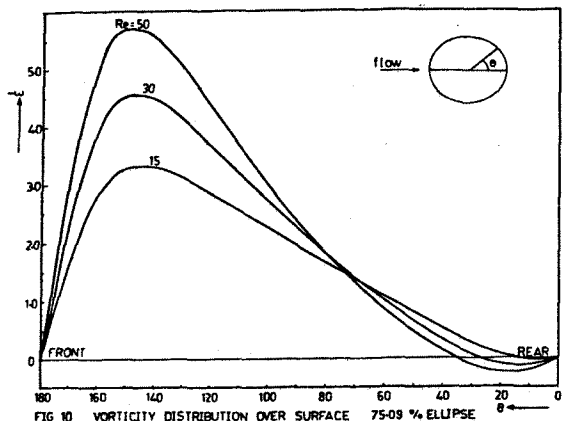


FIG 10 VORTICITY DISTRIBUTION OVER SURFACE 75.09% ELLIPSE

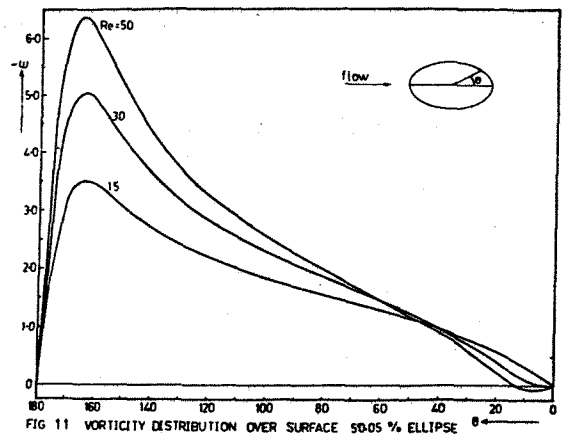


FIG 11 VORTICITY DISTRIBUTION OVER SURFACE 50.05% ELLIPSE

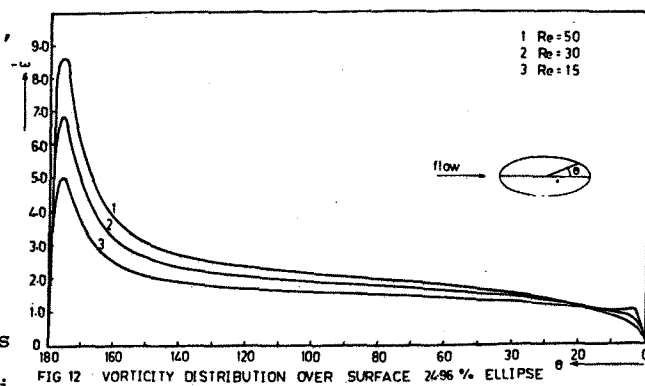


FIG 12 VORTICITY DISTRIBUTION OVER SURFACE 24.96% ELLIPSE

For incompressible, laminar steady flow in the Reynolds number range from 10 to 60, the decrease in coefficient of drag C_d , with increase in Reynolds number is due to both decrease in C_{dp} and C_{df} , i.e. coefficient of drag due to pressure and friction respectively. This change in C_{dp} and C_{df} is continuous more initially and less finally.

Discussion on Vorticity Distribution

Distribution of surface vorticity for the 99.93% elliptical cylinder at flow Reynolds number of 15 has been compared in fig.9 with the values obtained by Keller & Takami.

Data has been plotted for distribution of vorticity over the surface of 99.93%, 75.09%, 50.05% and 24.96% elliptical cylinders at Reynolds numbers of 15, 30 and 50. In figs. 9-12 respectively. These plots reveal, that the values of vorticity on the surface change sign in the hind region of 99.93% and 75.09% elliptical cylinders at Reynolds number of 50, 30 and 15; even for the 50.05% elliptical cylinder this behaviour persists at Re=50. A reversal in the sign of vorticity implies flow separation. At Re=30 and 15 for 50.30 and 15 for 24.96% elliptical cylinder there is no change in the sign of surface vorticity and obviously no separation of flow occurs.

Further for each of the elliptical cylinders, it is observed that maximum vorticity on the surface is at Reynolds number of 50, and lower values are observed at Reynolds number of 30 and still lower at Reynolds number of 15. The front stagnation point is at $\theta=180^\circ$ according to the coordinate system and based on the flow problem. At this point vorticity is zero. As the fluid moves along the curved surface of the elliptical cylinder from front stagnation point, vorticity is being generated along the surface. This vorticity is diffused in addition to being transported along the direction of flow for higher velocity flows and for creeping flows it is able to diffuse more in a direction transverse to the flow. Thus as the flow proceeds along curved surface the shear layer thickens due to retardation of flow near the body. With an increase in flow Reynolds number the vorticity on the surface of the elliptical cylinders is higher at higher Reynolds numbers. The magnitude of vorticity on the surface increases to a maximum value (figs 9-12) and then finally becomes zero at trailing edge, i.e., at $\theta=0^\circ$. For separated flow the vorticity value changes sign before it finally settles to zero value.

The maximum value of vorticity for 99.93% elliptical cylinder (refer fig.4) occurs for Re=15 at 125° , for Re=30 at 128.5° and for Re=50 at 130° . This occurrence of a maximum, upstream of 90° , in spite of the continued favourable pressure gradient is due to retarded flow and thickening of shear layer and its consequent effects. For higher Reynolds numbers the maximum vorticity point shifts towards upstream because of nature of favourable pressure gradient.

For 75.09% elliptical cylinder (refer fig. 10) the maximum value of vorticity occurs for Re= 15 at 145° , for Re=30 at 146.5° and for Re=50 at 148° . Then for 50.05% elliptical cylinder (refer fig.11) the maximum value of vorticity occurs for Re=15 at 164° for Re= 30 at 164° and for Re=50 and 165° ; and for 24.96% elliptical cylinder (refer fig.12) the

the maximum value of vorticity occurs at 175.5° for Re=15, 30 and 50. This clearly shows that the point of maximum vorticity shifts towards leading edge as the thickness of elliptical cylinder is decreased. Further it is observed that magnitude of maximum vorticity on the surface, for a given Reynolds number increases as the thickness ratio decreases below 75%.

Angle of Separation

The separation of flow on the surface of the cylinder takes place at zero vorticity point or where normal to the surface of body becomes tangential to velocity profile on surface. Fig.13 shows variation of angle of separation with Reynolds number. It is observed that angle of separation increases with increasing value of Reynolds number and decreases with decrease in thickness ratio. For the 24.96% elliptical cylinder there is no separation of flow in the given Reynolds number range. Further, good agreement exists between the predicted values of the angle of separation for 99.93% elliptical cylinder with those of circular cylinder.

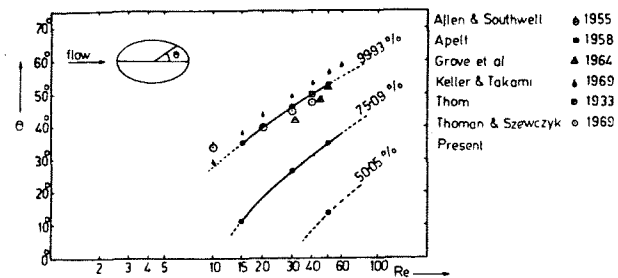


FIG 13 REYNOLDS NUMBER vs ANGLE OF SEPARATION

Discussion on Pressure Distribution:- Pressure distribution over surface for 99.93% elliptical cylinder at Re=15 is compared with pressure distribution over the surface of circular cylinder as obtained by Keller and Takami in fig.14. The results are found to be in good agreement. Flow over the surface of a solid body, in particular elliptical cylinder, is strongly influenced by the pressure distribution. The phenomenon of flow separation is intimately connected with the pressure distribution. For flow over a flat plate parallel to the flow stream, there is no separation of flow as there is very little or no pressure gradient. The distribution of pressure on the surface of elliptical cylinders can thus be considered to be made up in three zones:

- i) favourable pressure gradient - Zone I
- ii) slight favourable/adverse pressure gradient - Zone II.
- iii) Adverse pressure gradient - Zone III

For the 99.93% elliptical cylinder at $Re=15$ (fig.14), Zone I extends from 180° to 87° and for $Re=150$ from 180° to 93° .

Zone II of slight favourable/adverse pressure gradient is nearly absent. Zone III of adverse pressure gradient exists from 77° to 0° for $Re=50$. This clearly indicates that if flow separates for $Re=15$, then the point of separation shifts upstream with increase in Reynolds number to 30 and shifts still further upstream for Reynolds number of 50, and this does happen in the flow situation considered in the present computer experimentation(fig. 13 for angle of separation). The reason for different size of Zone I, Zone II, and Zone III for different elliptical cylinders (figs.14-17) may be attributed to (i) viscous effects which results in dissipation of energy of the system (ii) displacement thickness that alters the effective shape of the body for potential flow pressure distribution. These two factors are strongly influenced by Reynolds number and hence the size of zone changes with Reynolds number.

Then for the 24.96% elliptical cylinders (fig.17) it is seen that Zone I is very small, Zone II is larger, and Zone III is not existing. From this it may be inferred that the chances of flow separation diminish with decrease in thickness ratio. This pattern of pressure distribution on the surface may again be attributed to viscous effects and concept of displacement thickness.

Flow patterns

Stream lines and equivorticity lines are presented in figs. 18,19, and 20 for 24.96% elliptical cylinder at $Re=15$, 30 and 50 respectively.

a) Streamlines: The distance between two streamlines indicates the mass flow and thereby the velocity and tangent to a streamline gives direction of velocity; there is no velocity normal to a streamline. It is seen from fig. 18,19,20 that streamlines are deflected by the presence of the solid body and deflection corresponds to the shape of the body and Reynolds number. Thus velocities are higher ahead of cylinders and lower behind the cylinder.

The effect of increase in Reynolds number (from 15 to 30 and then to 50) is also noticed from figs. 18, 19 and 20. With increase in Reynolds number the streamlines ahead of cylinder becomes narrower while behind the cylinder get wider.

This means that velocities ahead of cylinders increase and behind the cylinders decrease with increase in Reynolds number. It was also seen from computer print outs which give velocities ahead and in wake

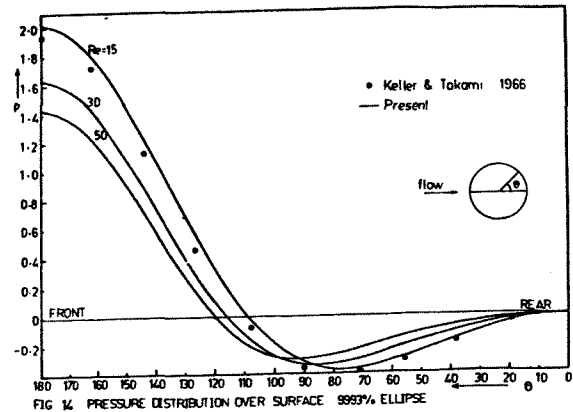


FIG 14 PRESSURE DISTRIBUTION OVER SURFACE 99.93% ELLIPSE

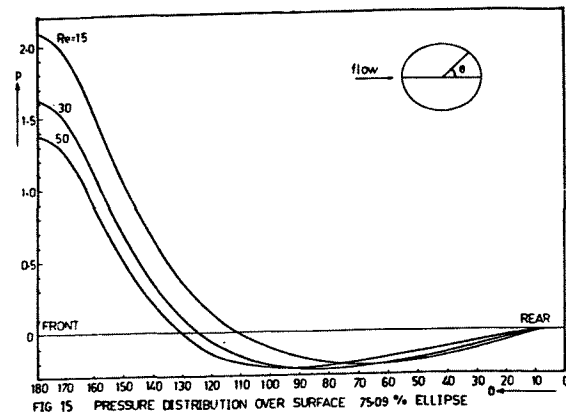


FIG 15 PRESSURE DISTRIBUTION OVER SURFACE 75.09 % ELLIPSE

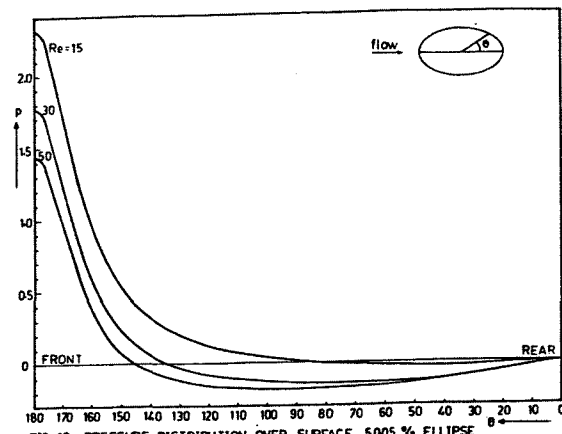


FIG 16 PRESSURE DISTRIBUTION OVER SURFACE 5.005 % ELLIPSE

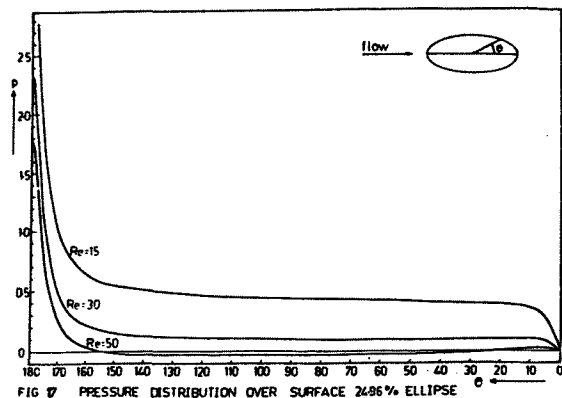


FIG 17 PRESSURE DISTRIBUTION OVER SURFACE 24.96% ELLIPSE

of 24.96% elliptical cylinder. The flow is unseparated in the case of 24.96% elliptical cylinder at $Re = 15, 30$ and 50 .

From velocity values for 99.93% elliptical cylinder, for 75.09% elliptical cylinder, for 50.05% elliptical cylinder it is clear that (i) velocity values ahead of elliptical cylinders are higher than velocity values in the wake. (ii) velocity values ahead of elliptical cylinders increase in Reynolds number, (iii) there is change in sign of velocity values in wake in case of separated flows.

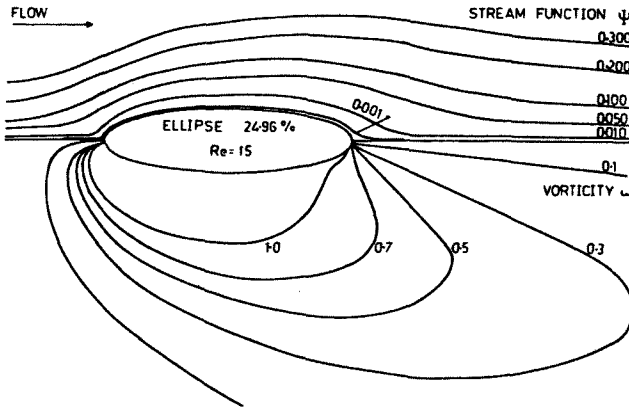


FIG 18 STREAM FUNCTION & VORTICITY DISTRIBUTION

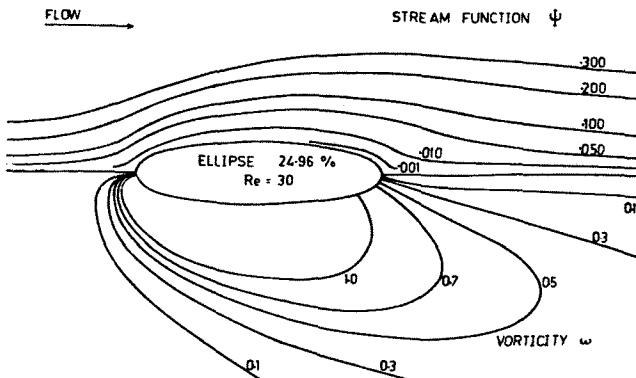


FIG 19 STREAM FUNCTION & VORTICITY DISTRIBUTION

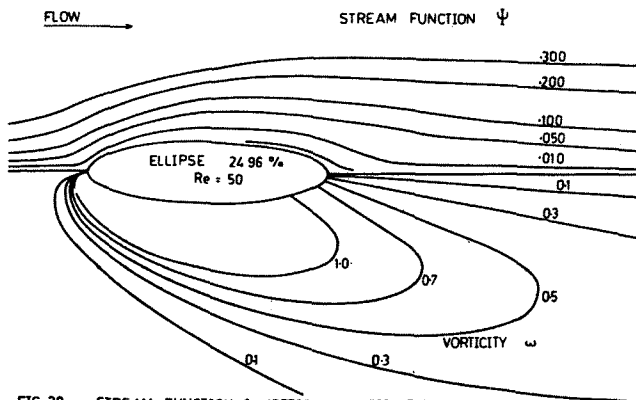


FIG 20 STREAM FUNCTION & VORTICITY DISTRIBUTION

b) Vorticity lines: Figs. 18,19 and 20 give the plots of equivorticity lines for 24.96% elliptical cylinders at Reynolds number of 15,30 and 50. With increase in Reynolds number the equivorticity lines are seen to elongate in the direction of flow. The vorticity concentration increases nearer the axis of symmetry and does not tend to spread, or, in other words the wake becomes narrower with increase in Reynolds number.

c) Velocity distribution: Velocity distribution on top surface, i.e., at $\theta = \pi/2$ given in computer print outs for 99.93% 75.09%, 50.05% and 24.96% elliptical cylinders respectively at Reynolds number of 15,30, and 50. From each of these tables(not given), it is seen that boundary layer thickness (i.e., where flow velocity is approximately 99% for free stream velocity) at the top at $\theta = \pi/2$ decreases with increase in Reynolds number. There is also decrease in boundary layer thickness due to increase in thickness ratio this happens due to favourable pressure gradient over larger portion of cylinders with higher thickness ratio and hence smaller boundary layer thickness at top of thicker cylinders.

VI. CONCLUSION

Navier Stokes equations have been solved for steady laminar and symmetric flow of viscous incompressible fluid over elliptical cylinders in the absence of body force. Solutions in terms of flow parameters have been obtained by solving finite difference form of disturbance stream function and vorticity transport equation. The technique used for obtaining solutions is a modification of extrapolated Liebmann method of successive over relaxation. Elliptic coordinate system has been used so that application of boundary conditions is easy and stretching of coordinates is not required. The distribution of grid points in the flow field is good, having more points at places where changes in dependent variables are significant in obtaining reasonable solutions, i.e., more points near leading and trailing edges and near the surface of the body.

By use of this coordinate system, problems can be solved for flow over bodies with geometrical shapes varying from flat plates to circular cylinders, the intermediate shapes being elliptical cylinders of different thickness ratio. The numerical scheme has been put to a more rigorous testing, i.e., results have been compared with existing results of circular cylinders (with separated flows) rather than comparisons with results of flat plates.

New type of boundary conditions have been developed, keeping in view the nature of laminar steady wake flow. These type of boundary conditions depict the flow correctly without the need to go too far from the body, thereby limiting the need to increase the grid points excessively and its subsequent effects, i.e. faster convergence.

The study of flow over elliptical cylinders has revealed that flow parameters are influenced by variation of Reynolds number and thickness ratio.

With increase in Reynolds number (i) the drag coefficient decreases more initially and lesser finally (as Reynolds number is further increased), (ii) the angle of separation increases, (iii) the length of recirculatory region increases linearly (iv) the maximum value of vorticity on the surface increases and this maximum value shifts towards leading edge as the thickness ratio is decreased, (v) the constant vorticity lines are elongated in the

direction of flow, and spreading of vorticity transverse to flow gets restricted to a narrower wake region, (vi) the boundary layer thickness at the top decreases and (vii) velocity values ahead of cylinder increases.

With increase in thickness ratio (i) drag coefficient increases linearly for thickness ratio greater than 25% (ii) Boundary layer thickness at the top decreases, (iii) there are higher chances of flow to separate, and in case of separated flows the angle of separation and length of recirculatory region increases.

An outcome of this research is development of 'drag thickness ratio law' by which values of drag coefficient for an elliptical cylinder can be estimated at a particular Reynolds number provided drag value of circular cylinder at that Reynolds number is known and thickness ratio of elliptical cylinder is more than 25%. There is some change in the nature of flow when the thickness ratio of elliptical cylinder becomes less than 25%,

Table 1 Summary of Calculations and results

THICKNESS RATIO	Re	r	ixj	C _{dp}	C _{df}	C _d	θ _s
99.93%	25	20	56x21	1.4504	0.9554	2.406	35°
	30	20	56x21	1.0828	0.5834	1.666	46°
	50	20	56x21	0.8866	0.4012	1.288	53°
75.09%	15	22	56x21	1.2894	0.9654	2.254	11°
	30	22	56x21	0.9332	0.5888	1.522	27°
	50	22	56x21	0.7404	0.4038	1.142	35°
50.05%	15	28	56x21	1.0990	0.9624	2.062	-
	30	21	56x21	0.8032	0.6106	1.414	-
	50	21	56x21	0.6190	0.4188	1.038	13.3°
24.96	15	21	56x21	0.9798	1.0244	2.004	-
	30	21	56x21	0.6518	0.6258	1.287	-
	50	21	56x21	0.4812	0.4302	0.911	-

REFERENCES

1. Harrison, W.J.; On the Motion of Spheres, Circular and Elliptic Cylinders Through Viscous Liquids", Trans, Camb.Phil. Soc. 23,1924.
2. Wang, C.W., Separation and Stall of an Impulsively Started Elliptic Cylinder, J. Appl. Mech., n 34,p.823 1967.
3. Taneda, S., Lift on Implusively Started Elliptic Cylinders, J.Phys. Soc. Japan, n 33, p. 1706, 1972.
4. Lugt, H.J. and Haussling, H.J., Laminar Flow Past an Abruptly Accelerated Elliptic Cylinder at 45° Incidence JFM, n 65, P 711, 1974.
5. Lugt, H.J. and Ohring, S., Laminar Flow Behaviour under Slip Boundary Conditions, Phys. Fluids, n 28, pl, 1975.
6. Thom, A., The Flow Past Circular Cylinders at Low Speeds, Proc. Roy Soc. London A, n 141, p.651, 1933.
7. Kawaguti, M., Numerical Solution of the Navier Stokes Equations for the Flow Around a Circular Cylinder at Reynolds Number 40, J.Phys. Soc. Japan, n 8, p 747, 1953.
8. Apelt, C.J., The Steady Flow of a Viscous Fluid Past a Circular Cylinder at Reynolds Numbers 40 and 44. ARC RM & B No. 3175, 1961.
9. Allen, D.N. de G, and Southwell, R.V. Relaxation Methods Applied to Determine the Motion in Two Dimensions of a Viscous Fluid Past a Fixed Cylinder. Quart. J.Mech. Appl.Math, n8,p.129,1955.
10. Hamielec, A.E. and Raal, J.D., Numerical Studies of Viscous Flow Around Circular Cylinders, Phys. Fluids, V12 n1, p11,1969.
11. Keller, H.B. and Takami, H, Numerical Studies of Steady Viscous Flow About Cylinders. Numerical Solutions of Non-linear Differential Equations. Edited by Greenspan, D.John Wiley & Sons, Inc., p. 115,1969.
12. Dennis, S.C.R. and Chang G.Z., Numerical Solutions for Steady Flow Past a Circular Cylinder at Reynolds Numbers upto 100. J. Fluid Mech.,n42, p.471, 1970.
13. Underwood , R.L., Calculations of Incompressible Flow Past a Circular Cylinder at Moderate Reynolds Numbers J. Fluid Mech., n 37, p.95, 1969.
14. Fornberg, B., A Numerical Study of Steady Viscous Flow Past a Circular Cylinder, J.Fluid Mech.V98,p.819, 1980.
15. Payne, R.B., Calculation of Unsteady Viscous Flow Past a Circular Cylinder J. Fluid Mech, n 4,p 81, 1958.
16. Jain, P.C. and Kawaguti, M., Numerical Study of a Viscous Fluid Flow Past a Circular Cylinder, J.Phys. Soc. Japan V.21, n 10, p.2055, 1966.
17. Ingham, D.B., Note on the Numerical Solution of Unsteady Viscous Flow Past a Circular Cylinder, J.Fluid Mech., n 31, p. 815, 1968.
18. Jain P.C. and Rao, K.S., Numerical Solution of Unsteady Viscous Incompressible Fluid Flow Past Circular Cylinder, Phys. Fluids, V12, n 12,p.57 II, 1969.
19. Thoman, D.C. and Szewczyk, A.A., Time Dependent Viscous Flow Over a Circular Cylinder, Phys. Fluids, V.12, n 12, p.76 II, 1969.
20. Dey, S.K. Numerical Studies of the Navier Stokes Equations with Applications to a Circular Cylinder, Ph.D. Thesis, Mississippi State University College of Engineering, State College Mississippi, 1970.
21. Lin, S.P. and Gautesen, A.K., Initial Drag on a Cylinder, Quart. J.Mech. Appl. Math, n 29, p 61, 1976.
22. Son, J.S. and Hanratty, T.J., Numerical Solution for the Flow Around a Cylinder at Reynolds Number of 40, 200, 500, J. Fluid Mech, n 35, p 369, 1969.
23. Taneda, S., Experimental Investigation of the Wakes Behind Cylinders and Plates at Low Reynolds Numbers, J. Phys. Soc. Japan, VII n 33, 1956.
24. Tritton, D.J., Experiments on the Flow Past a Circular Cylinder at Low Reynolds Numbers, J. Fluid Mech, n 19, p.547, 1959.
25. Grove, A.A., Shair, F.H. , Peterson, E.E., Acrivos, A., An experimental Investigation of the Steady separated Flow Past a Circular Cylinder, J.Fluid Mech, n 19, p.60, 1964.
26. Coutanceau, M., and Bouard, R., Experimental Determination of the Main Features of the Viscous Flow in the Wake of a Circular Cylinder in Uniform Translation (Steady Flow part I), J. Fluid Mech., V79, p 231, 1977.

27. Jordan, S.K. and Fromm, J.E., Laminar Flow Past a Circle in a Shear Flow Phys. Fluid, V15, n6, p 972, 1972.
28. Patel, V.A., Time Dependent Solutions of the Viscous Incompressible Flow Past a Circular Cylinder by the Method of Series Truncation, Comp., Fluids 4, p 13, 1976.
29. Fornberg, B., Steady Viscous Flow Past a Circular Cylinder upto Reynolds Number 600, J. Comput, Phys., n 53, p.42, 1985.
30. Temperton, C., On the FACR (I) Algorithm for the Discrete Poisson Equation J. Comput. Phys., n 34, p 314, 1980.
31. Berger, B.S., Asymptotic Approximation and Perturbation Stream Functions in Viscous Flow Calculations, ASME J. Appl. Mech., n 52, p. 190, 1985.
32. Peregrine, D.H., A Note on the Steady High Reynolds Number Flow About a Circular Cylinder, J.Fluid Mech., n 157, p.493, 1985.
33. Smith F.T., Laminar Flow of an Incompressible Fluid Past a Bluff Body: the Separation, Reattachment, Eddy Properties and Drag, J. Fluid Mech, n 92, p 171, 1979.
34. Smith, F.T., A Structure for Laminar Flow Past a Bluff Body at High Reynolds Number, J. Fluid Mech. n 155, p 175,.1985.
35. Ghia, K.N., Ghia, U., Osswald, G.A., Liu, C.A. ' Simulation of Separated Flow Past a Bluff Body Using Navier Stokes Equations'. Boundary Layer Separation IUTAM Symposium, London, 1986. Springer- Verlag Berlin 1987 .p 251.
36. Imai, I., On the Asymptotic Behaviour of Viscous Fluid Flow at a Great Distance from a Cylindrical Body wit Special Reference to Filon's Paradox, Proc. Roy.Soc. London A, n 208, p 487, 1951.
37. Bahl., R., Incompressible Viscous Flow Over Elliptic Cylinders, Ph.D. Thesis, Faculty of Engineering and Technology, Panjab University, Chandigarh, India, 1982.